Research Article

Journal of Environmental Nanotechnology

Synthesis, Characterization and Biological Activity Studies of Semicarbazone Ligand

B. Karpagam[1*], J. Rajesh[2], G. Rajagopal[3]

[1]Department of Chemistry, St. Michael College of Engineering and Technology, Kalayarkoil, Sivagangai, TN, India
[2]Department of Chemistry, Saveetha School of Engineering, Saveetha University, Chennai, TN, India
[3]Department of Chemistry, Chikkanna Government Arts College, Tiruppur, TN, India
Received: 10.01.2021 Accepted: 05.03.2021 Published: 30-06-2021
*karpagamsentil@gmail.com

ABSTRACT

The ligand 1-(3-ethoxy-2-hydroxybenzilidene-4-phenylsemicarbazide), (L1) was synthesized and characterized with the help of Infra-red, Ultra-violet, ^{1}H NMR spectroscopy and X-ray crystallography. The spectral data also indicate that the ligand coordinates through the phenolic oxygen and the azomethine nitrogen atoms. Crystal data revealed that the semicarbazone act as bidentate ligand, making use of azomethine nitrogen atom and oxygen atom for co-ordination to the central metal atom. The Ligand L1 have been screened for their antibacterial activity against gram-positive bacterium *Staphylococcus aureus* and gram-negative bacteria *Escherichia coli and Pseudomonas aeruginosa*. The ligand L1 exhibited appreciable activity against gram-positive bacteria *Staphylococcus aureus* and it is resistant to fungal species such as *Candida albicans*, *Aspergillus niger and Macrophonia phaseolina*. The free ligand L1 also shows higher IC_{50} values against MCF-7 cells indicating less anticancer activity.

Keywords: Antibacterial and anti-tumor activity; Semicarbazone; X-ray crystallography.

1. INTRODUCTION

Semicarbazone plays a key role in organic and biological chemistry. The semicarbazone linkage is an important functional group due to its extensive presence in natural products, pharmaceutical compounds and synthetic polymers. The most common traditional method for the synthesis of the semicarbazone derivative is that semicarbazide hydrochloride on treatment with pyruvic acid or acetone gives semicarbazone derivative. In recent years, there has been considerable interest in the study of semicarbazone due to their coordination modes when bound to the metal. The anticancer activity of certain pyridoxal semicarbazone (3-hydroxyl-5-hydroxymethyl-2- methyl-4-pyridine-carboxaldehyde semicarbazide) has also been studied. The coordinating ability of semicarbazones to both transition and main group metallic cations is attributed to the extended delocalization of electron density over the semicarbazone skeleton, which is enhanced by substitution at N(4)-position.

Condensation of semicarbazides with aldehydes or ketones extends the electron delocalization along with the azomethine bond. 2-hydroxybenzaldehyde N(4)-substituted semicarbazones, as well as heterocyclic thiosemicarbazones, derived from the presence of several potential donor atoms, their flexibility and their ability to coordinate in either neutral or deprotonated forms, have been the subject of extensive investigations because of their ability to strongly coordinate metal ions as bidentate ligands and their broad spectrum of biological applications (Leovac *et al.* 2014). Due to their good complexing properties, biological activity and analytical application, semi-/thiosemi-/isothio-semicarbazides and their Schiff bases of different denticity, as well as their metal complexes, have been the subject of many studies. The most numerous among them are the complexes with bi/tridentate salicylaldehyde semi/thiosemi-/isothiosemicarbazones (Ahmed *et al.* 2015).

Semicarbazones and thiosemicarbazone of salicylaldehyde (Kalaivani *et al.* 2012; Hossain *et al.* 2017) and their derivatives are of a class of versatile ON/ONS donors capable of stabilizing both higher and lower oxidation states of transition metal ions (Pahontu *et al.* 2015; Selvaganapathy *et al.* 2016). Although capable of deprotonation at both the phenol and thioamide functions to give a dianionic ligand, they can also act as monoanionic chelating ligands, coordinating to a metal centre phenolic oxygen, the thione sulfur and azomethine nitrogen (Haque *et al.* 2015). The dianionic form of the ligand is favored at higher through the deprotonated pH, whereas the monoanionic form is promoted at low pH. However, the coordination chemistry of substituted or unsubstituted semicarbazones and thiosemicarbazones of salicylaldehyde is quite unexplored in the previous reports (Kumar *et al.* 2015). This prompted our study into the synthesis and characterization of substituted semicarbazones using

aromatic aldehydes and its metal complexes. Here we have synthesized the new semicarbazone ligand using 3-Ethoxy salicylaldehyde and 4-Phenylsemicarbazide.

This paper describes the synthesis of semicarbazone ligand (L1), and various physico-chemical methods employed for the characterization of the newly synthesized semicarbazone ligand and its biological applications.

2. EXPERIMENTAL PROCEDURE

2.1 Synthesis of Semicarbazone Ligand L1

About 499 mg (3.00 mmol) of 3-Ethoxy salicylaldehyde in 5 ml methanol was treated with 454 mg (3.00 mmol) of 4-phenylsemicarbazide in 5 ml methanol and stirred for 2 hours. Then it is refluxed for 3 hours in a round-bottom flask. The solution was chilled (overnight) and fine colorless needles of the compound separated out. The solution was filtered washed well with cold methanol. The compound was recrystallized from methanol and dried in vacuo over P_40_{10} (Scheme 1).

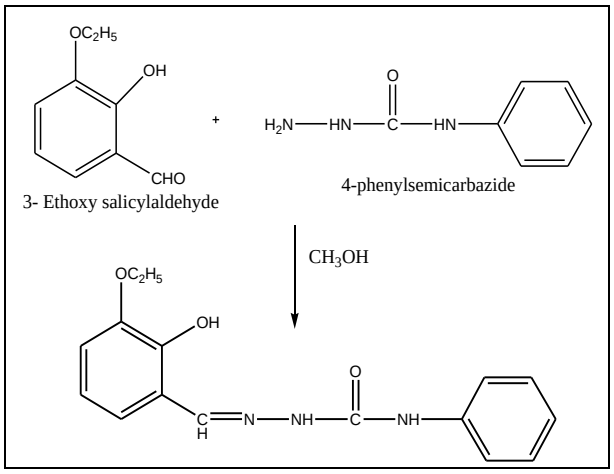

Scheme 1: Synthesis of Semicarbazone ligand L1

3. RESULTS AND DISCUSSION

The newly synthesized semicarbazone ligand is characterized by using single-crystal X-ray diffraction, IR spectra, electronic spectra and ^{1}H NMR spectra.

3.1 X-Ray Crystallography

The structure of semicarbazone Ligand L1 with thermal ellipsoids at 50% probability was shown in Fig. 1. The present compound crystallizes in the monoclinic system with C2/C space group (Table 1). There is only one molecule in the asymmetric unit (Fig. 2). The bond lengths and bond angles of the molecules are presented in Table 2. In the present structure, the atoms N_1 and O_3 are in trans conformation with respect to N2 -C_8 bond (Fig. 3) by the torsion angle O_3-C_8-N_2-N_1 =176.50 as in the structure of salicylaldehyde N(4)-Phenylthiosemicarbazone (Seena *et al.* 2008) and 2-hydroxyacetophenone (4)cyclohexythiosemicarbazone (Strehler *et al.* 2015). It is also supported by the bond lengths C_8-O_3 =1.22 and C_8-N_2 =1.3633. C_8-O_3 bond length is the double bond length. But N_1-N_2 =1.3699 and C_8-N_2 =1.3633 are intermediate between single and double bonds as in the structure of salicylaldehyde N(4)–Phenylthiosemicarbazone (Seena *et al.* 2008). O_3 atom is trans to the hydrozinic N_1 atom as in the structures of salicylaldehyde semicarbazone (Enyedy *et al.* 2014), Benzaldehyde semicarbazone salicylaldehyde thiosemicarbazone (Pahontu *et al.* 2013). The mean deviation calculations show that the semicarbazone moiety C_7-N_1-N_2-C_8-O_3-N_3 is nearly planar with a deviation 0.293 at C_7 and -0.0393 at N_1. Ring puckering and least square plane analysis show that the rings are in the same plane and these rings have not deviated from the central semicarbazone moiety.

3.2 Hydrogen Bonding

The present structure is stabilized by both inter and intramolecular hydrogen bonds (Fig. 1). The intramolecular hydrogen bonds are C_{10}-H_{10}….O_3 & O_1-H_{10}….O_2.The lists of hydrogen bonds present in the structure ar e given in Table 3. The imine N atom is not involved in the hydrogen bonding with O_1 of phenyl ring since the N_1 atom are in trans conformation with O_1. The hydrogen bonds N_2-H_2N…O_1 (-x+1,-y+1,-z) and O_1-H_1…O_3 (-X+1,-Y+1,-Z) formed a closed-loop R^2_2 (5) andN_2-H_2N…O_1 hydrogen bond itself formed an R^2_2(14) hydrogen bonding motif.

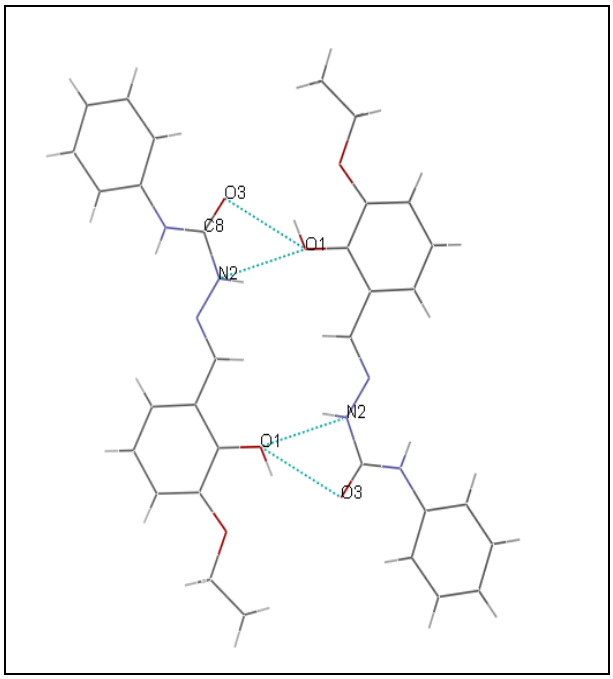

Fig. 1: Structure of semicarbazone Ligand L1

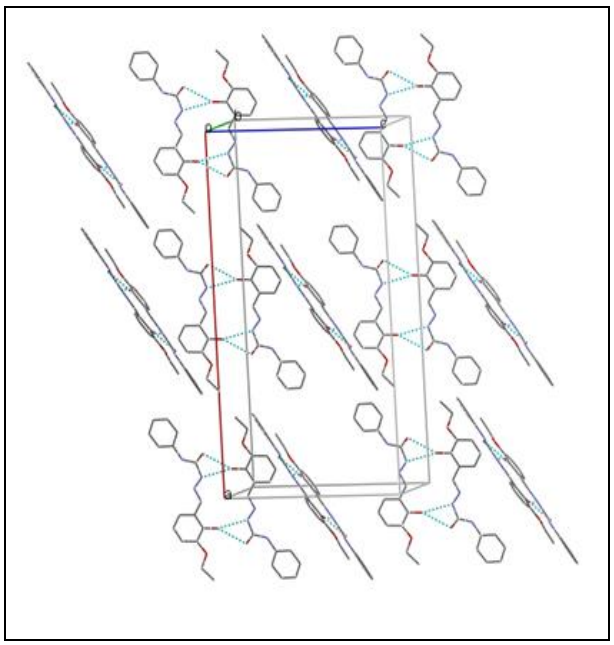

Fig. 2: Unit cell packing diagram of semicarbazone L1

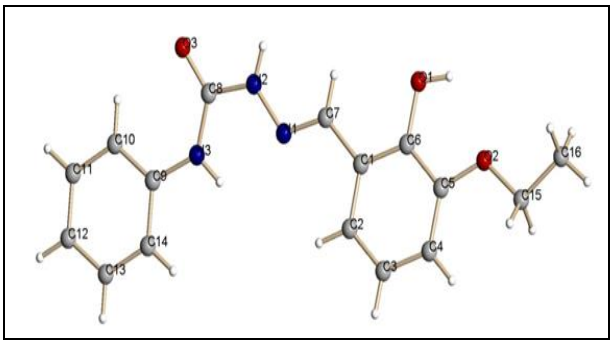

Fig. 3: Monomeric structure of the semicarbazone ligand

Table 1. Crystal data and structure refinement for thiosemicarbazone ligand 1

Crystal data	**Ligand 1**
Empirical Formula	$C_{16}H_{17}N_3O3$
Formula weight	299.33
Wavelength Aº	0.71073
Crystal system	monoclinic
Space group	C2/C
A, b, c [Angstrom]	30.131(2), 5.5670(4), 18.2336(15)
Alpha, beta, gamma [deg]	90, 92.660(2), 90
V [Ang ^{**3}]	3055.2(4)
Z Value	8
D(calc) [g/cm^{**3}]	1.301
F(000)	1264
Absorption coefficient mm^-1	0.092
Temperature K	294(2)
Theta Min-Max [Deg]	2.24 to 25.00
Completeness to theta	25.00 99.9%
Refinement method	Full matrix least-square on F^2
Final R indices [I>2sigma(I)]	R1 = 0.0349, wR2 = 0.0970
R indices (all data)	R1=0.0465, wR2=0.1104
Largest diff. Peak and hole e.A^{-3}	0.138 and -0.104

Table 2. Selected Bond lengths [A] and angles [deg] for L1

Atoms	**Bond length**
C(5)-O(2)	1.3703 (17)
C(6)-O(1)	1.3635(16)
C(7)-N(1)	1.2762(16)
C(8)-O(3)	1.2264(17)
C(8)-N(3)	1.3533(18)
C(8)-N(2)	1.3632(18)
C(9)-N(3)	1.4105(17)
C(15)-O(2)	1.4246(18)
N(1)-N(2)	1.3701(17)
N(2)-H(2N)	0.840(18)
N(3)-H(3N)	0.860(17)
O(1)-H(1)	0.88(2)

Table 3. Selected Bond lengths [A] and angles [deg] for Ligand1

Atoms	Bond angle
O(2)-C(5)-C(4)	126.64(13)
O(2)-C(5)-C(6)	113.35(12)
O(1)-C(6)-C(1)	119.26(12)
O(1)-C(6)-C(5)	120.01(12)
N(1)-C(7)-C(1)	122.47(12)
N(1)-C(7)-H(7)	118.8
O(3)-C(8)-N(3)	125.82(13)
O(3)-C(8)-N(2)	119.87(13)
N(3)-C(8)-N(2)	114.31(13)
C(7)-N(1)-N(2)	115.78(12)
C(8)-N(2)-N(1)	122.75(12)
C(8)-N(3)-C(9)	128.36(12)
C(6)-O(1)-H(1)	109.7(13)
C(5)-O(2)-C(15)	118.79(12)

3.3 IR Spectra

IR spectra of L1 show bands at 3315 and 3390 cm^{-1} regions due to intermolecular hydrogen-bonded phenolic - OH groups (Table 4). It also suggests that the ligand exists in enol form in the solid-state (Ravoof *et al.* 2010) present in the molecule. The azomethine stretching vibrations, C=N, characteristics of a Schiff and the coordination mode of ligand are supported by the disappearance of these bands in the spectra of complexes (Shimazaki *et al.* 2011; Abu-Khadra *et al.* 2016). The ligand has bands in the range of 2546 - 2900 cm^{-1} due to - NH groups base, are observed at ~ 1681 cm^{-1} (Sumrra *et al.* 2014; Shirode, P. R., Yeole *et al.* 2014). The carbonyl group shows stretching and bending vibrations at ~ 1319 and 887 cm^{-1}, while additional bands in the broad region of 1543-748 cm^{-1} are due to vibrations involving interactions between C=O stretching and C—N stretching attached to a nitrogen atom (Mandal *et al.* 2016). Medium bands observed in the range 1064 -1149cm^{-1} are assigned to hydrazinic N—N bonds (Mangamamba *et al.* 2014). The 1681-1450 cm^{-1} region of the spectra is complicated by the presence of ring breathing vibrations of the phenyl rings (Fig.4).

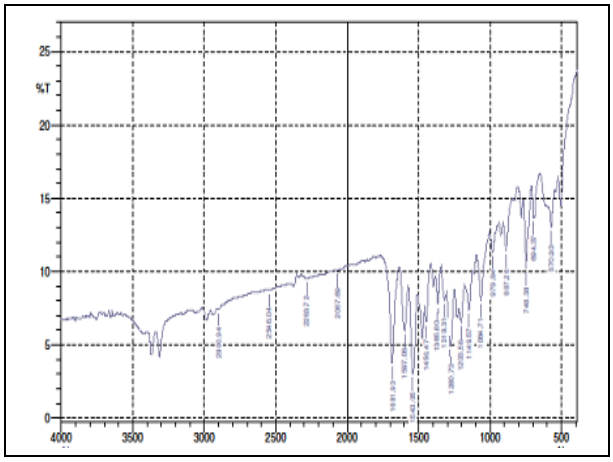

Fig.4. IR spectra of the newly synthesized ligand (L1)

Table 4. IR spectral data (cm^{-1}) and UV spectral data (nm) of free ligand (L1)

Ligand 1	Compound
1543	$\upsilon_{(CH=N)}$
1280	$\upsilon_{(C-O)}$
3390	$\upsilon_{(N-H)}$
748	$\upsilon_{(C=S)}$
3315	$\upsilon_{(O-H)}$
---	$\upsilon_{(M-N)}$
---	$\upsilon_{(M-O)}$
291 - 332	λ_{max} (nm)

3.4 Electronic Spectra

In contrast to the infrared spectrum, the electronic spectrum is not used primarily to identify individual functional groups but rather to show the relationship between functional groups, chiefly conjugation. The electronic spectral data of the ligand in DMF solution are presented in Table 5. The π—>π* transitions of the phenyl ring are observed in the 263-291 nm region (Fig.5). The n→π* transitions of the imine function of the semicarbazone moiety are observed in the region of 301-332nm (Goel *et al.* 2013).

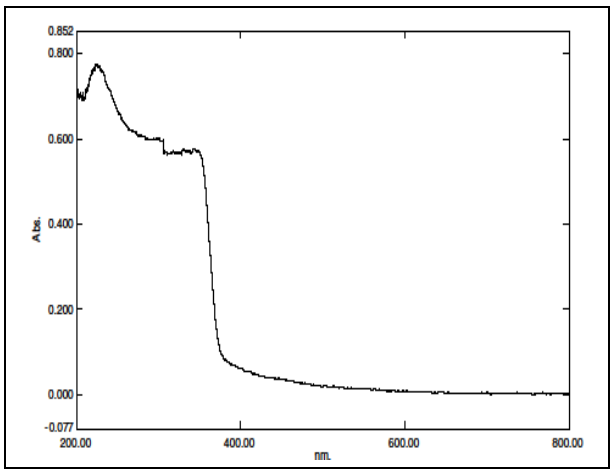

Fig. 5: Electronic spectrum of the ligand (L1)

3.5 ^{1}H NMR Spectra

Proton Magnetic Resonance spectroscopy is a helpful tool for the preparation of organic compounds in conjugation with other spectrometric information. The ^{1}H NMR spectra of the ligand were recorded in $CDCl_3$ (Table 5). The ligand does not show any peak attributable to -SH proton, but they show peaks assignable to the secondary N-H protons. In the spectra of the ligand, sharp singlets at 7.64 and 8.29 ppm are due to CH proton (Fig.6). Absence of any coupling interactions by ^{2}NH due to the unavailability of protons on neighboring atoms renders a singlet peak for the imine proton at 8.87ppm. The $^{a}CH_2$ protons adjacent to the ring nitrogen produce a triplet at 4.02ppm due to coupling with nearby $^{b}CH_2$ protons. The $^{b}CH_2$ protons due to coupling with $^{a}CH_2$ and $^{c}CH_2$ protons resonate as the multiplet observed at 1.38 ppm. The OCH_3 protons appear as a singlet at 3.37 ppm. The spectra of the ligand (L1) also show sharp singlets, which integrate as one hydrogen at ~ 10.67 ppm is assigned to the proton attached to the oxygen atom. The downfield shift of this proton is assigned to its intra and intermolecular hydrogen-bonding interactions. The hydrogen bonding decreases the electron density around the proton and thus moves the proton absorption to a lower field. Absence of any coupling interactions by ^{2}NH due to the unavailability of protons on neighboring atoms renders a singlet peak for the imine proton at 8.87ppm. The presence of an electron-withdrawing azomethine group near the ^{7}CH proton leads to its resonance as a singlet at 7.64 ppm. Aromatic protons ^{4}CH, ^{6}CH, ^{3}CH, ^{5}CH appear as a multiplet in the range of 6.76-7.31 ppm. NMR assignments are in agreement with values already reported.

3.6 Anion Sensing Analysis

3.6.1 Colorimetric Analysis

In order to deduce the anion sensing ability of the sensor (L1) with halide anions (F^-, Cl^-, Br^- and I^-), experiments were carried out in different solvents, namely $CHCl_3$, CH_3CN and DMSO. The change in optical and optoelectronic properties was monitored by visual (naked-eye). First, the halide anions (F^-, Cl^-, Br^- and I^-) were added as tetrabutylammonium salts (0.2 equiv) to solutions of the sensor (L1) in chloroform/acetonitrile/DMSO. In the naked eye experiments, the sensor (L1) (5×10^{-5} M) showed a dramatic color change from colorless to pale yellow in the presence of tetrabutylammonium fluoride (0.2 equiv) (Fig.7). The reason for this color change was probably due to the formation of hydrogen bond interactions between the two NH groups of the ligand and fluoride ions. The receptor was insensitive even on the addition of significant excess of Cl^-, $Br^-$and I^- (up to 100 equiv). No color change ($CHCl_3$ and DMSO medium) was observed in the presence of chloride, bromide and iodide ions as similar to acetonitrile medium. In the receptors, it has been speculated to be a hydrogen bond-donor and suitable to interact with the anions, has been appended in between substituted-aldehyde and amine units.

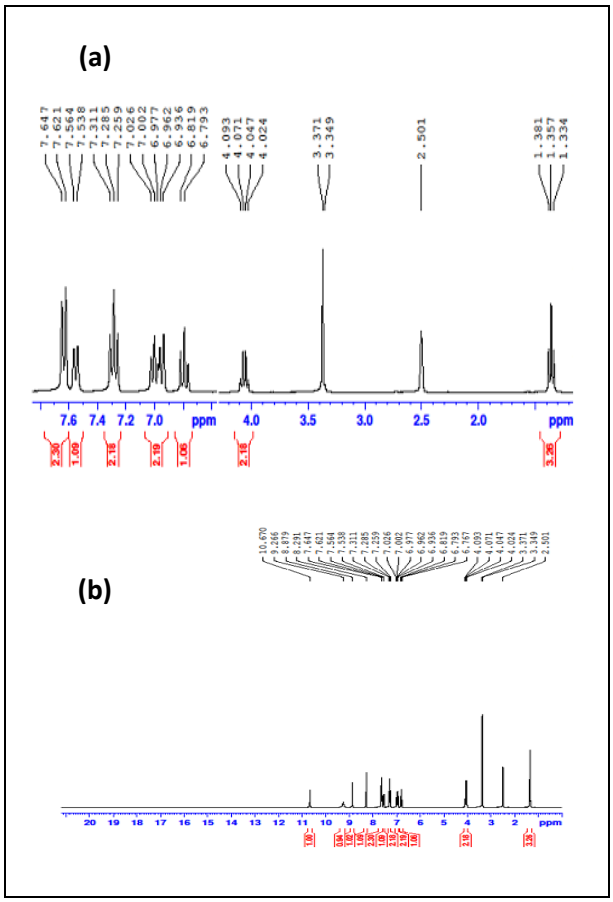

Fig. 6: (a) ^{1}H NMR spectrum of the ligand in $CDCl_3$- d_6 (b) Expanded form of L1

The covalently linked 4-phenylthiosemicarbazone moiety intends to act as a chromospheres unit (Li *et al.* 2012). The experimental results indicate that this receptor is highly selective compared with similar motifs and

sensitive to recognize fluoride anion in dry CH_3CN and the processes of sensing can be obviously seen through the visible color changes for naked-eye recognition.

Table 5. ^{1}H NMR spectral data of the L1 (in ppm)

Ligand 1	Compound
10.67	υ (O-H)
8.87	υ (CH=N)
6.76 – 7.31	Aromatic
3.34 – 3.37	Aliphatic

Fig. 7: Color changes of sensor (L=L1) (5.0×10$^-$5 M) in CH_3CN before and after addition of 0.2 equiv of representative anions (from left to right:L,L+F^-, L+Br^-, L+Cl^-, L+I^-, L+Aco^-, L+ CN^-)

3.6.2 UV Kinetics

The interaction of sensor 1 with the fluoride anion was investigated through spectrophotometric titrations by adding a standard solution of tetrabutylammonium salt of the anion in acetonitrile of the free receptor and for the titration of sensor 1 with F^-, was shown in Fig.8. The titrations were carried out in CH_3CN at 5.0×10^{-5}M of L1 upon the addition of incremental amounts of 0.02 ml (5.0×10^-4 M) of tetrabutylammonium fluoride and the changes in UV–Vis spectra are observed. In the absence of anions, the UV–Vis absorption spectrum of 1 was characterized by the presence of four absorption maxima. The first two bands (210–280 nm) could be assigned to excitation of the p-electrons of the aromatic system, the third band, 315 nm is due to the transition between the p-orbital localized on the azomethine group (CH=N). The band in the region of 405 nm may occur due to intramolecular charge-transfer transitions within the whole structure of the Schiff base. Upon addition of F^-, a dramatic change in the spectra was observed. The peaks at 315 and 405 nm of the free receptor gradually decrease and a new absorption peak appears at 460 nm, as the concentration of F^- increases due to the formation of a complex with the receptor. A bathochromic (red) shift of the absorption maxima (460 nm) in the visible region of the spectra was observed on the complexation of receptors with F^-. This is presumably due to charge transfer after the interaction between the proton of the amine group and the acceptor (anion) groups (El-Asmy *et al.* 2009; Ghosh *et al.* 2011).

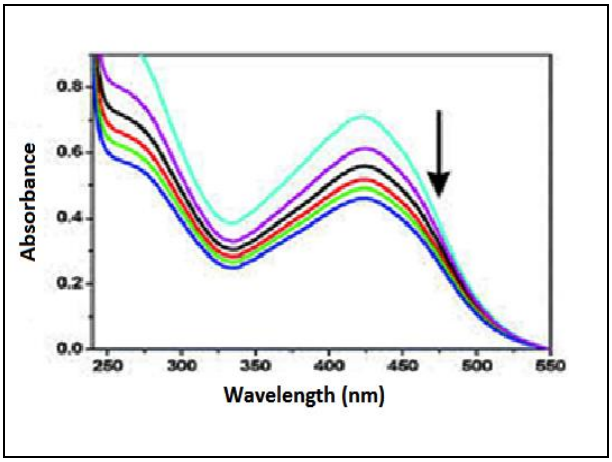

Fig. 8: The changes in the absorption spectra of L1 (5×10^{-5}M) upon addition of F^-(0 -100 equiv) in CH_3CN, demonstrating that the anion can interact with semicarbazone moiety, giving rise to large changes in the ground state properties of the sensor.

3.7 Biological Studies

3.7.1 Antibacterial Activity

The newly synthesized Ligand was tested for their antibacterial activity by measuring the inhibition area on agar plates (diffusimetric method) with the standard drug Amikacin were screened separately for their antibacterial activity against the gram-positive bacteria *Staphylococcus aureus* and Gram-negative bacteria *Escherichia coli* and *Pseudomonas aeruginosa*. The results of the antibacterial activity of semicarbazone Ligand were listed in table 6 as estimated by a zone of inhibition (mm). The results show that free semicarbazone ligand (L1) have effective activity against Gram-positive bacteria *Staphylococcus aureus and shows resistivity against* Gram-negative bacteria *Escherichia coli* and *Pseudomonas aeruginosa* (Fig.9)

3.7.2 Antifungal Activity

Table 6 indicates that the ligand **(**L1**)** has a lower degree of antifungal activity against *Candida albicans*, *Aspergillus niger* and *Macrophonia phaseolina* at 2 mg/ ml concentration. The effect is susceptible to the concentration of the compound used for inhibition. The antifungal experimental results of the compounds were compared with the standard antifungal drug Ketokonazole at the same concentration. From the observed data (Table 6) it shows that the antifungal activity of the ligand (L1**)** shows resistance against the fungal species (Fig.9a).

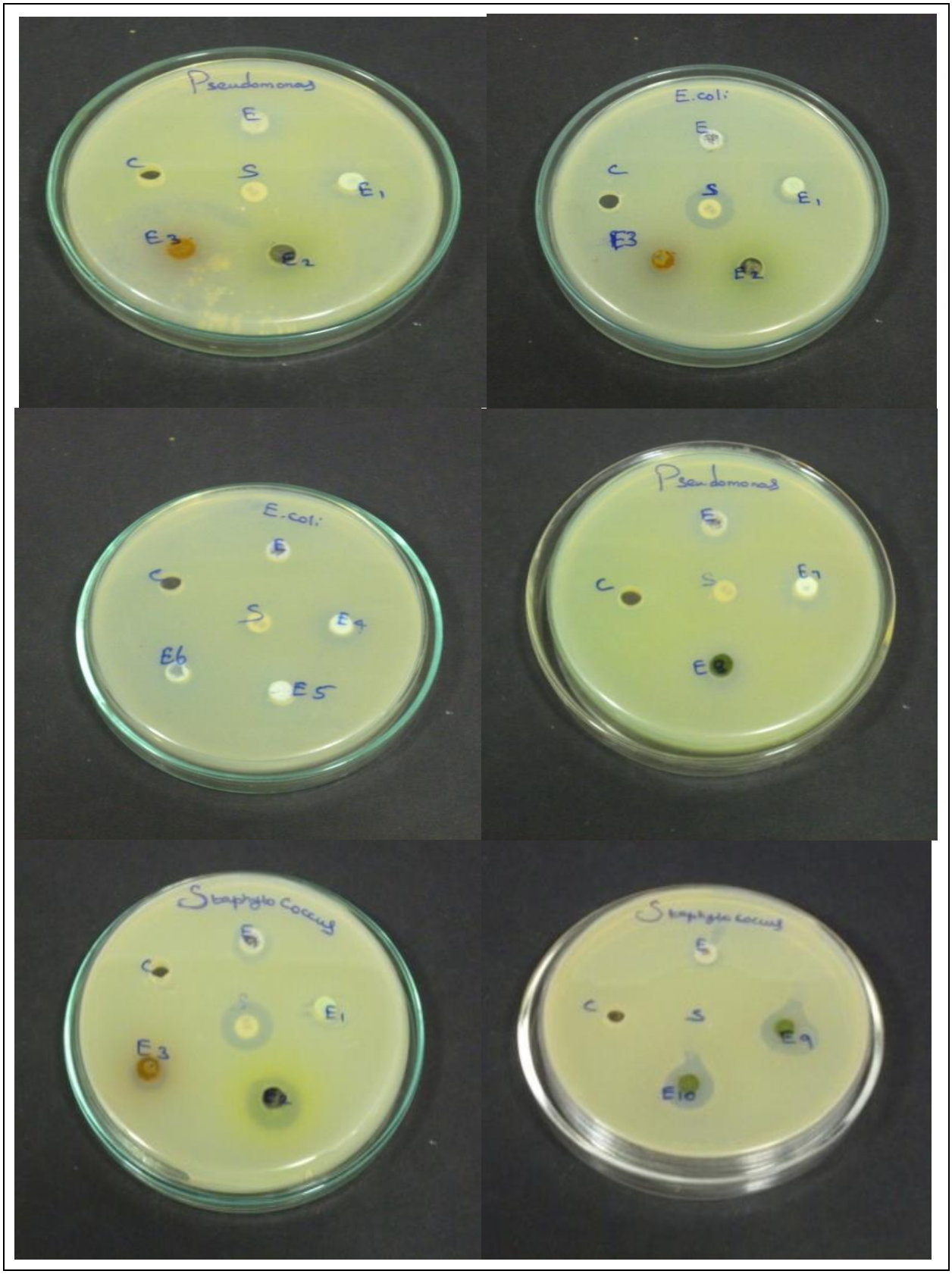

Fig. 9: Images of zone of inhibition in ligand L1 against bacteria

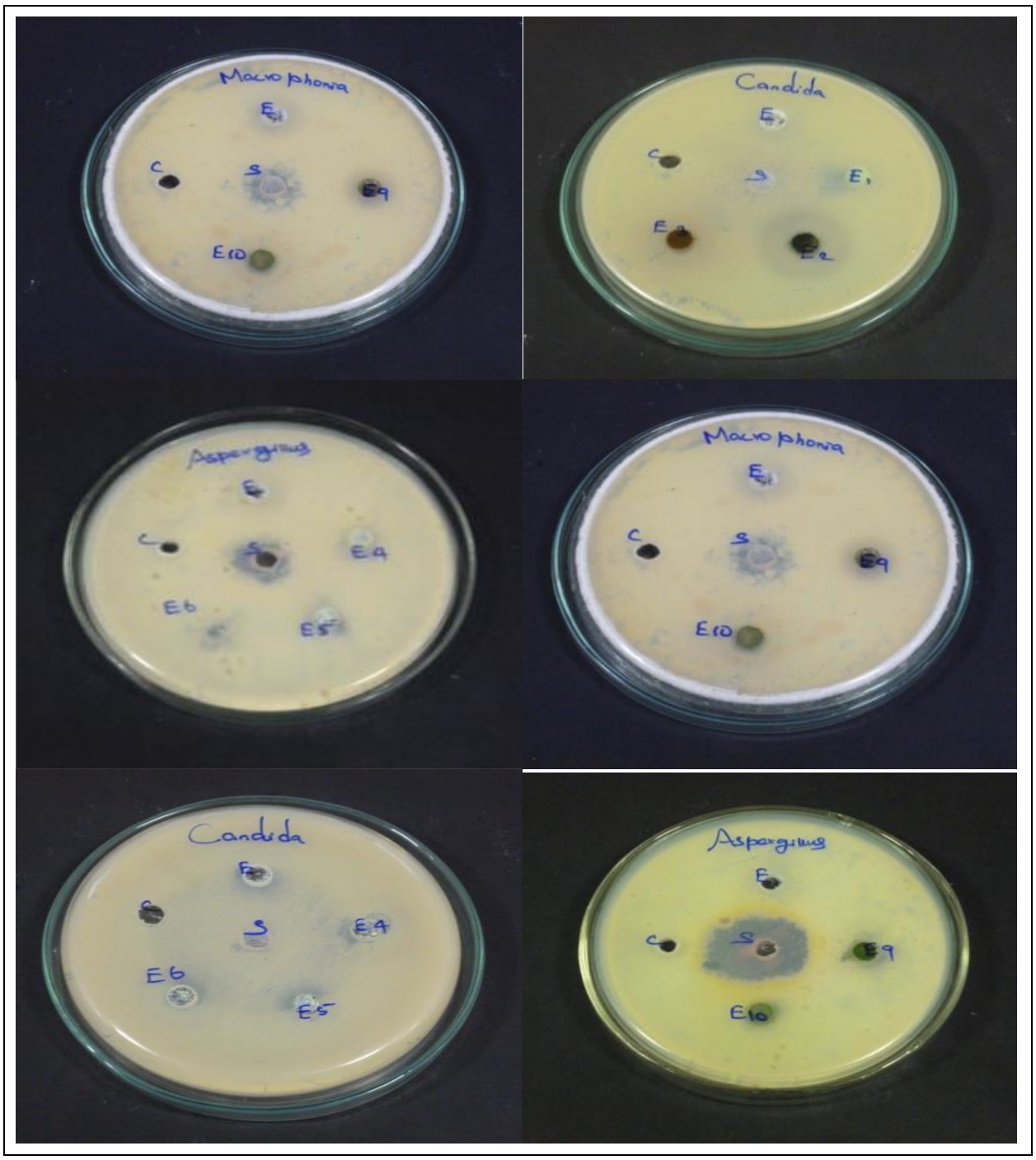

Fig. 9: (a) Images of Zone Inhibition in ligand (L1) against fungi

Table 6. Antimicrobial activity of the newly synthesized Semicarbazone ligand (L1)

Sample	*E.coli*	*Staphylococcus aureus*	*Pseudomonasauroginosa*	*Candidaalbicans*	*Aspergillusniger*	*Macrophonia phaseolina*
Ligand 1	R	4	R	R	R	R
STANDARD	17	18	17	21	17	15

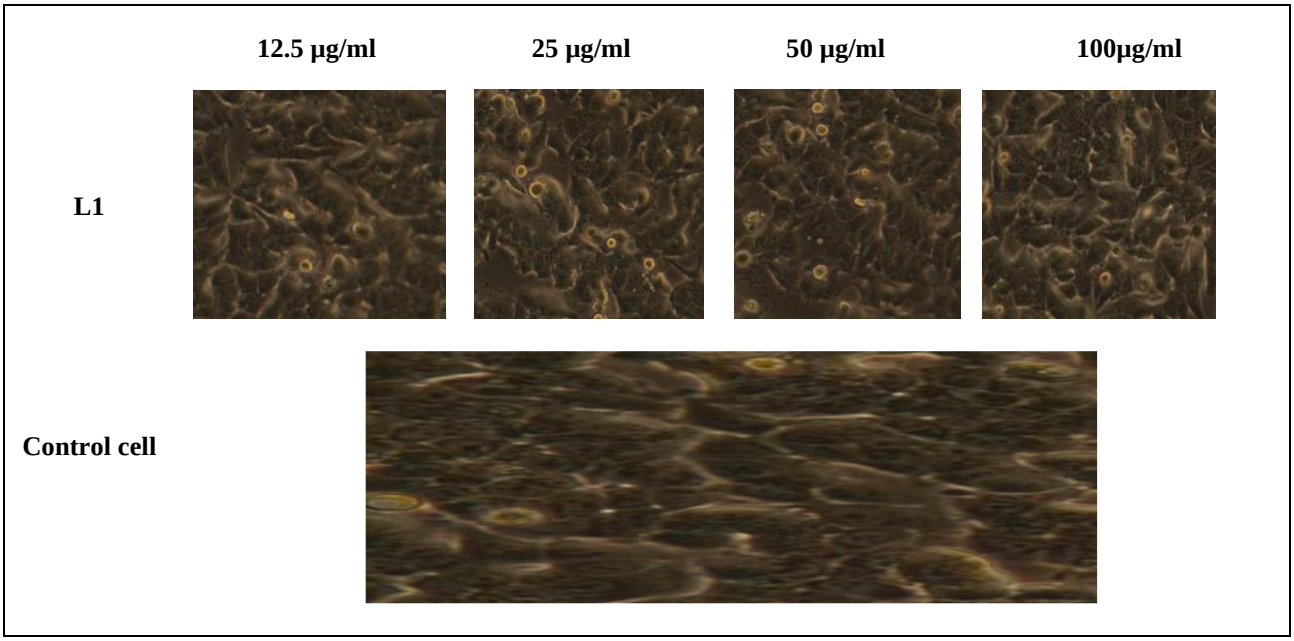

Fig. 9.1: Morphological changes in MCF-7 cells incubated for 24 h compound of ligand.

The cells are observed under a phase contrast microscope × 100.

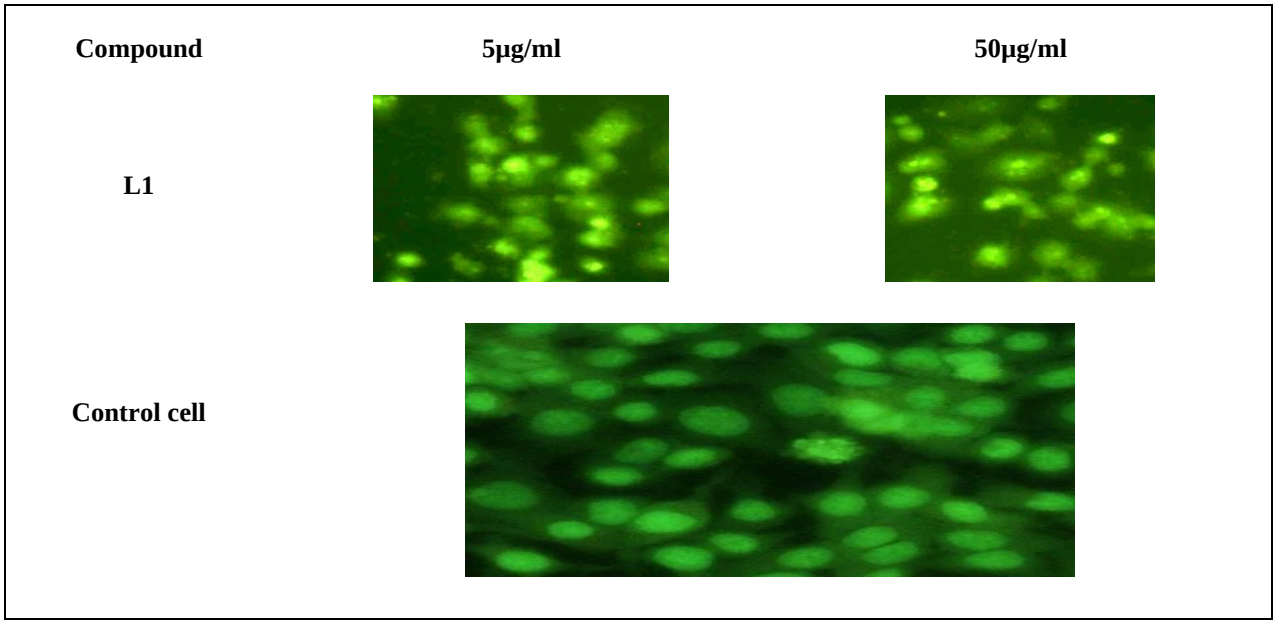

Fig. 9.2: Fluorescent Staining Studies of the synthesized ligand (L1) and control cell

Table 7. IC_{50} values of the ligand L1

S. No	Sample	IC_{50} values
1.	Ligand 1	112
2.	Cyclophosphamide	100

3.8 Invitro Cytotoxic Activity

The *in vitro* cytotoxic activities of the synthesized Schiff base ligand (L1) were studied on human breast cancer cell lines (MCF-7) by applying the MTT colorimetric assay (Table 7). IC_{50} values (compound concentration that produces 50% of cell death) were calculated for the free ligand. Cyclophosphamide is chosen as a reference compound. It is worth noting that the free ligand shows higher IC_{50} values, indicating that

the antitumor activity of the free ligand shows lesser activity against human breast cancer cell lines (MCF-7).

3.9 Fluorescent Staining Studies

Apoptosis (programmed cell death) is a normal component of the development and maintenance of the health of multicellular organisms. Cells die in response to a variety of external and physiological stimuli, and during apoptosis, they do so in a controlled and regulated fashion. This makes apoptosis distinct from the other form of cell death, namely, necrosis in which uncontrolled (accidental) cell death leads to lysis of cells, inflammatory responses and potentially serious health problems. Moreover, apoptosis, by contrast, is a process in which cells play an active role in their own death (cell suicide). Most tumor cells retain their sensitivity to some apoptotic stimuli from chemotherapeutic agents, and in this context, the apoptosis-inducing ability of drugs seems to be a primary factor in determining their efficacy.

In the present study, the characteristic morphological changes induced by the ligand L1 have been evaluated by adopting fluorescent microscopic analysis of Acridine orange/EthBr (AO/EB)-stained cells. Upon treatment of the cells with IC_{50} concentration of L1 at different incubation times 24 hrs, morphological changes such as chromatin fragmentation, bi- or multinucleation, cytoplasmic vacuolation, nuclear swelling, cytoplasmic blebbing, and late apoptosis indication of dot-like chromatin condensation have been observed by adopting AO/EB staining. All the morphological changes observed for the ligand L1 suggest that the cells are committed to death in such a way that both apoptotic and necrotic cells increase in number in a time-dependent manner (Fig.9.2).

4. CONCLUSION

1- (3- ethoxy-2-hydroxy benzilidene -4-phenylsemicarbazide) the ligand L1 has been prepared and characterized by spectral techniques and X-ray crystallography. The spectral data also indicate that the ligand coordinates through the phenolic oxygen and the azomethine nitrogen atoms. Crystal data revealed that the semicarbazone acts as bidentate ligand, using the azomethine nitrogen atom and oxygen atom for co-ordination to the central metal atom. Further, in the anion sensing analysis, the color change seen with the naked eye is probably due to hydrogen bond interactions between the two NH groups of the ligand and fluoride ions. The antibacterial activity results show that free semicarbazone ligand (L1) has effective activity against gram-positive bacteria *Staphylococcus aureus* and it is resistant to the fungal species. The free ligand L1 also shows higher IC_{50} values against MCF-7 cells indicating less anticancer activity.

SUPPLEMENTARY DATA

CCDC 923703 contains the supplementary crystallographic data for 3-(ethoxy-2-hydroxybenzylidene)-4-phenylsemicarbazide. These data can be obtained free of charge via http://www.ccdc.cam.ac.uk/conts/retrieving.html, or from Cambridge Crystallographic Data Centre, 12 Union Road, Cambridge CB2 1EZ, UK; Fax: +44 1223 336 033; or e-mail: deposit@ccdc.cam.ac.uk.

FUNDING

This research received no specific grant from any funding agency in the public, commercial, or not-for-profit sectors.

CONFLICTS OF INTEREST

The authors declare that there is no conflict of interest.

REFERENCES

Abu-Khadra, A. S., Farag, R. S. and Abdel-Hady, A. E.-D. M., Synthesis, Characterization and antimicrobial activity of Schiff base (E)-N-(4-(2-Hydroxybenzylideneamino Phenylsulfonyl) acetamide metal complexes, *Am. J. Anal. Chem.*, 07(03), 233–245 (2016). https://dx.doi.org/10.4236/ajac.2016.73020

Ahmed, N., Riaz, M., Ahmed, A. and Bhagat, M., Synthesis, characterisation, and biological evaluation of Zn(II) complex with tridentate (NNO Donor) schiff base ligand, *Int. J. Inorg. Chem.*, 2015, 01–05 (2015). https://dx.doi.org/10.1155/2015/607178

El-Asmy, A. A. and Al-Hazmi, G. A. A., Synthesis and spectral feature of benzophenone-substituted thiosemicarbazones and their Ni(II) and Cu(II) complexes, *Spectrochim. Acta Part A Mol. Biomol. Spectrosc.*, 71(5), 1885–1890 (2009). https://dx.doi.org/10.1016/j.saa.2008.07.005

Enyedy, É. A., Bognár, G. M., Nagy, N. V., Jakusch, T., Kiss, T. and Gambino, D., Solution speciation of potential anticancer metal complexes of salicylaldehyde semicarbazone and its bromo derivative, *Polyhedron*, 67, 242–252 (2014). https://dx.doi.org/10.1016/j.poly.2013.08.053

Ghosh, K., Adhikari, S., Fröhlich, R., Petsalakis, I. D. and Theodorakopoulos, G., Experimental and theoretical anion binding studies on coumarin linked thiourea and urea molecules, *J. Mol. Struct.*, 1004(1–3), 193–203 (2011). https://dx.doi.org/10.1016/j.molstruc.2011.08.004

Goel, S., Chandra, S. and Dwivedi, S. D., Spectroscopic and biological studies on newly synthesized Cobalt (II) and Nickel (II) complexes with 2-Acetyl coumarone semicarbazone and 2-Acetyl coumarone thiosemicarbazone, *J. Chem.*, 2013, 01–07 (2013). https://dx.doi.org/10.1155/2013/742915

Haque, R. A. and Salam, M. A., Synthesis, structural characterization and biological activities of organotin (IV) complexes with 5-allyl-2-hydroxy-3-methoxybenzaldehyde-4-thiosemicarbazone, *J. Chem. Sci.*, 127(9), 1589–1597 (2015). https://dx.doi.org/10.1007/s12039-015-0924-9

Hossain, S., Zakaria, C. M. and Kudrat-E-Zahan, Structural and biological activity studies on metal complexes containing thiosemicarbzone and isatin based schiff base: A review, *Asian J. Res. Chem.*, 10(1), 6 (2017). https://dx.doi.org/10.5958/0974-4150.2017.00002.5

Kalaivani, P., Prabhakaran, R., Poornima, P., Dallemer, F., Vijayalakshmi, K., Padma, V. V., Natarajan, K., Versatile Coordination Behavior of Salicylaldehydethiosemicarbazone in Ruthenium(II) Carbonyl Complexes: Synthesis, Spectral, X-ray, Electrochemistry, DNA Binding, Cytotoxicity, and Cellular Uptake Studies, *Organometallics*, 31(23), 8323–8332 (2012). https://dx.doi.org/10.1021/om300914n

Kumar, B., Kumar, R., Kumar, B., Magnetic and Spectral Study of Some Mixed Ligand Complexes, *Orient. J. Chem.*, 31(3), 1827–1830 (2015). https://dx.doi.org/10.13005/ojc/310366

Leovac, V., Vojinovic-Jesic, L., Ivkovic, S., Rodic, M., Jovanovic, L., Holló, B., Mészáros-Szécsényi, K., Transition metal complexes with thiosemicarbazide-based ligands. Part 60. Reactions of copper(II) bromide with pyridoxal S-methylisothiosemicarbazone (PLITSC). Crystal structure of [Cu(PLITSC−H)H_2O]Br•H_2O, *J. Serbian Chem. Soc.*, 79(3), 291–302 (2014). https://dx.doi.org/10.2298/JSC130622084L

Li, S., Cao, X., Chen, C., Ke, S., Novel salicylic acid-oriented thiourea-type receptors as colorimetric chemosensor: Synthesis, characterizations and selective naked-eye recognition properties, *Spectrochim. Acta Part A Mol. Biomol. Spectrosc.*, 96, 18–23 (2012). https://dx.doi.org/10.1016/j.saa.2012.04.102

Mandal, S., Saha, R., Saha, M., Pradhan, R., Butcher, R. J., Saha, N. C., Synthesis, crystal structure, spectral characterization and photoluminescence property of three Cd(II) complexes with a pyrazole based Schiff-base ligand, *J. Mol. Struct.*, 1110, 11–18 (2016). https://dx.doi.org/10.1016/j.molstruc.2016.01.020

Mangamamba, T., Ganorkar, M. C., Swarnabala, G., Characterization of Complexes Synthesized Using Schiff Base Ligands and Their Screening for Toxicity Two Fungal and One Bacterial Species on Rice Pathogens, *Int. J. Inorg. Chem.*, 2014, 01–22 (2014). https://dx.doi.org/10.1155/2014/736538

Pahontu, E., Fala, V., Gulea, A., Poirier, D., Tapcov, V., Rosu, T., Synthesis and Characterization of Some New Cu(II), Ni(II) and Zn(II) Complexes with Salicylidene Thiosemicarbazones: Antibacterial, Antifungal and in Vitro Antileukemia Activity, *Molecules*, 18(8), 8812–8836 (2013). https://dx.doi.org/10.3390/molecules18088812

Pahontu, E., Julea, F., Rosu, T., Purcarea, V., Chumakov, Y., Petrenco, P., Gulea, A., Antibacterial, antifungal and in vitro antileukaemia activity of metal complexes with thiosemicarbazones, *J. Cell. Mol. Med.*, 19(4), 865–878 (2015). https://dx.doi.org/10.1111/jcmm.12508

Seena, E. B., Prathapachandra Kurup, M. R., Suresh, E., Crystal Study of Salicylaldehyde N(4)-Phenylthiosemicarbazone, *J. Chem. Crystallogr.*, 38(2), 93–96 (2008). https://dx.doi.org/10.1007/s10870-007-9268-8

Selvaganapathy, M., Raman, N., Pharmacological Activity of a Few Transition Metal Complexes: A Short Review, *J. Chem. Biol. Ther.*, 1(2), 108 (2016). https://dx.doi.org/10.4172/2572-0406.1000108

Shimazaki, Y., Arai, N., Dunn, T. J., Yajima, T., Tani, F., Ramogida, C. F., Storr, T., Influence of the chelate effect on the electronic structure of one-electron oxidized group 10 metal(ii)-(disalicylidene)diamine complexes, *Dalt. Trans.*, 40(11), 2469-2479 (2011). https://dx.doi.org/10.1039/c0dt01574a

Shirode, P. R., Yeole, P. M., Synthesis and Characterization of Mixed Ligand Complexes of transition metals with Schiff's bases, *Chem. Sci. Trans.*,3(3), 1186-1192 (2014). https://dx.doi.org/10.7598/cst2014.801

Strehler, F., Korb, M., Lang, H., Crystal structure of paddle-wheel sandwich-type [Cu_2 {$(CH_3)_2$ CO}{μ-Fe(η^5-$C_5H_4C{\equiv}N)_2$}$_3$]$(BF_4)_2$·$(CH_3)_2CO$, *Acta Crystallogr., Sect. E: Crystallogr. Commun.*, 71(2), 244–247 (2015). https://dx.doi.org/10.1107/S2056989015001760

Sumrra, S. H., Ibrahim, M., Ambreen, S., Imran, M., Danish, M., Rehmani, F. S., Synthesis, Spectral Characterization, and Biological Evaluation of Transition Metal Complexes of Bidentate N, O Donor Schiff Bases, *Bio. Inorg. Chem. Appl.*, 2014, 01–10 (2014). https://dx.doi.org/10.1155/2014/812924